NJC

Accepted Manuscript

This is an *Accepted Manuscript*, which has been through the Royal Society of Chemistry peer review process and has been accepted for publication.

Accepted Manuscripts are published online shortly after acceptance, before technical editing, formatting and proof reading. Using this free service, authors can make their results available to the community, in citable form, before we publish the edited article. We will replace this *Accepted Manuscript* with the edited and formatted *Advance Article* as soon as it is available.

You can find more information about *Accepted Manuscripts* in the Information for Authors.

Please note that technical editing may introduce minor changes to the text and/or graphics, which may alter content. The journal's standard Terms & Conditions and the Ethical guidelines still apply. In no event shall the Royal Society of Chemistry be held responsible for any errors or omissions in this *Accepted Manuscript* or any consequences arising from the use of any information it contains.

ROYAL SOCIETY OF CHEMISTRY

www.rsc.org/njc

Journal Name

RSCPublishing

ARTICLE

Graphene Grown in Situ on TiO_2 Hollow Nanocrystals for Advanced Photocatalysis and Lithium-Ion Batteries

Cite this: DOI: 10.1039/xoxxoooooox

Jicai Liang [ab], Juan Wang[a], Yi Li [a], Meixin Zhou[a], Xiaofeng Wang[c] , Xiangji Li[b] and Kaifeng Yu[a*]

Received ooth January 2012,
Accepted ooth January 2012

DOI: 10.1039/xoxxoooooox

www.rsc.org/

Graphene nanosheets (GAs) grown on TiO_2 hollow nanocrystals have been successfully fabricated for the first time via a simple one-step hydrothermal method for advanced photocatalysis and lithium ion batteries. The current study has shown that the nanocomposite materials can better decomposition organic pollutants and can provide the additional electron transport pathways implying a significant potential application for photocatalysis and LIBs. The nanocomposite materials have showed highly active photocatalysis, a high rate capability, and stable cycling. Furthermore, the nanocomposite materials with 1% graphene exhibit the greatest photoelectrical properties and Li-ion insertion/extraction kinetics in TiO_2.

1. Introduction

Hollow micro-/nanostructures are of great interest in many current and emerging areas of technology. In a growing number of applications, including catalysts, hydrogen production and storage, photonics, photovoltaics, drugs, and rechargeable batteries, the hollow micro-/nanostructures play important roles in determining function.[1]

Up to now, a group of templating methods have been proven very effective and gifted for synthesizing a varity of hollow structures. Therefore, the hollow nanostructure of titanium dioxide is becoming more and more attractive as advanced photocatalyst and electrode materials for lithium-ion batteries (LIBs) because it is photochemical stability, low toxicity and relatively cheap, compared with other semiconductors.[2,3] The practical application range of TiO_2 can be greatly extended to self-cleaning development owing to its excellent photocatalytic activity.[4] However, the photocatalytic activity is usually unsatisfactory , because most of the light-generated electron-hole pairs of TiO_2 cannot be separated or transferred in time, which leads to poor efficiency of photocatalysis. The reported attempts to avoid the recombination of electrons and holes is based on the doping of titanium dioxide with noble metals such as Pt、Au、and Pd,[5,6] and non-metallic doping.[7] In particular, various types of carbonaceous nanomaterials, including activated carbon,[8] carbon nanotube[9] are used to modify TiO_2.

Graphene, a one-atom-thick sp^2-hybridized carbon sheet, has attracted a great deal of scientific interest since its discovery by Geim and co-workers.[10] Owing to its outstanding mechanical, electrical, and thermal properties,[11,12] graphene holds enormous potential in a variety of applications. In addition, its unique nanostructure, large theoretical specific surface area (~2600m^2/g),[13] high elasticity,[14] hydrophobic properties and chemical stability make graphene a promising nanoscale building block for preparing composites. The hollow structure of TiO_2/GAs can provide more Li-ion transfer channels, providing an ideal negative electrode material well suited for LIBs.[15] The TiO_2/graphene or TiO_2/reduced graphene oxide (RGO) composites are commonly synthesized via the reaction of graphene oxide (GO) and TiO_2 nanoparticles via hydrothermal reaction,[16] UV photocatalytic reduction of GO in the presence of TiO_2,[17] dispersion of graphene in sol–gel.[18] In this work, instead of using TiO_2 nanoparticles directly for the preparation of the composite, we propose a facile one-pot hydrothermal route to synthesize TiO_2/graphene composite using titanium sulfate as the precursor. In this way, the size of the TiO_2 could be well controlled and the restacking of graphene could be effectively prevented. Most importantly, the in situ formed TiO_2, intermediates and graphene might construct layered structure or mesoporous structure that is beneficial to specific capacity and rate performance of the LIBs.[19, 20] Therefore, we report a simple one-step hydrothermal template-free method towards in situ growth of TiO_2 nanospheres on GO. Importantly, photocatalytic performance and electrochemical properties of the hybrid materials can also be tuned easily by adjusting the weight ratio of graphene of mixture.

2. Results and Discussion

2.1. Morphology and structure characterization

The crystalline structure of GO, GAs-TiO_2 and TiO_2 was analyzed by powder X-ray diffraction (XRD). As shown in Fig.1, GO has a diffraction peak centered at 2θ=11.4° corresponding to the (001) reflection with interlayer spacing of 7.75Å,[21] It shows the XRD profiles of G-TiO2 hybrids and TiO_2 have diffraction peaks at 2θ values of 25.2°, 37.8°, 48.0°, 54.7 °and 62.5°, which derive from (101), (004), (200), (211) and (204) reflexes of TiO_2 anatase, respectively.[22] In contrast to the standard pattern of anatase phase, the XRD profile of TiO_2 on GR exhibits an extreme peak intensity and narrow width for the (101) reflex, and a comparatively low

diffraction intensity for the (004), (200), (211) and (204) reflexes, indicating the formation of TiO_2 on GR sheets with the preferred growth orientation along the c-axis of anatase lattice. Furthermore, after the growth of TiO_2, the feature diffraction peak of the GO (001) plane (11.7°) has disappeared, due to the full exfoliation of the graphite oxide, indicating the GO is reduced to GAs on this occasion.

Typical morphology of the GAs/TiO_2 (1.0 wt. %) along with the bare GO and black TiO_2 for comparison shown in the transmission electron microscopy (TEM) image of Fig. 2 and Fig.3. From Fig. 2, it is observed that GO has a flake-like structure with wrinkles, which is consistent with the results reported by other groups.[23, 24] The Fig.2b shows that GO is consist of several layers instead of single layer. Although it is very difficult to obtain monolayer graphene in 3D GAs, our results show that the conductivity and photocatalytic properties of TiO_2/GAs are far better than those of blank TiO_2 hollow nanocrystals.

Fig. 3a and b are low-magnification TEM images of TiO_2/GAs (1.0 wt. %) showing that some uniform nanoparticles dispersed on the GO materials, and the TiO_2/GAs maintain the hollow sphere structure as the same to pure TiO_2, The spherical dark contrast on the outer rim of each particle is consistent with the shell structure .The high-resolution TEM image (Fig. 3c) reveals well-defined lattice fringes of TiO_2 nanoparticle, corresponding to the (101) plane of anatase TiO_2, and the diameter of TiO_2 hollow nanocrystals is smaller than 20 nm and the diameter of the hollow part is approximately 3 to 5 nm.

The morphology of TiO_2/GAs was further observed with SEM. It was easy to find many platelets of TiO_2/GAs composites, along with large aggregated TiO_2 hollow nanocrystals (Fig.4). For a single platelet, TiO_2 nanoparticles deposited on graphene oxide sheets had a diameter of 20–40 nm.

Fourier-transform infrared (FTIR) spectroscopic study shows the spectrum of GO and G1-TiO_2. The characteristic absorption bands of GO[25] (1730.8 cm^{-1} for C=O stretching, 1393.4 cm^{-1} for C–OH stretching, 3422.6 cm^{-1} for O–H stretching) are absent, and in contrast the skeletal vibration at 1625.4 cm^{-1} attributed to the aromatic C=C group in G_1-TiO_2 spectrum appears, suggesting that GO was primely reduced to graphene. Moreover, an unobvious absorption peak at around 798 cm^{-1} in the spectrum of G1-TiO_2 assigned to the Ti–O–C vibration was observed.[26] The results suggest that Ti atoms of TiO2 can interact with the graphene to form chemisorption interfaces via Ti–O–C bonding. The presence of Ti–O–C band indicates that this method ensures good TiO_2−graphene contact through chemical bonds, favoring the charge transfer between TiO_2 and graphene upon light excitation.

2.2. Photocatalytic performance

Methylthionine chloride was selected as a model organic pollutant to evaluate the photocatalytic performance of the TiO_2/GAs composite. Before the photocatalytic experiment, the suspension was magnetically stirred for 30 min in dark to achieve the adsorption–desorption equilibration to discount the adsorption of the substrate on the catalyst. The rapid degradation of methylthionine chloride over the graphene oxide/TiO_2 compositions was clearly seen from the change of UV–vis absorption spectra of the solution in the course of the degradation. From the Fig.5, It is clearly seen that in the tested concentration range, any addition of graphite oxide in the synthesis solution resulted in TiO_2/GAs composites showing much better photocatalytic activity than the TiO_2 alone, The photocatalytic activities of TiO_2 and G–TiO_2 series were measured in terms of the degradation efficiency (%) of Methylthionine chloride by the following equation:

$$\text{Degradation efficiency (\%)} = \frac{C_0 - C_i}{C_0} * 100$$

Where C_0 is the initial concentration of MB and Ci is the concentration of MB solution after UV or visible light irradiation. The order of photo degradation of Methylthionine chloride under UV irradiation is as follows: G_1–TiO_2 > G_2–TiO_2 > $G_{0.5}$–TiO_2 > G_5–TiO_2 > TiO_2. Due to the unique electronic transport property of graphene and more transports from the TiO_2 hollow nanocrystals, the electrons stimulated by light from TiO_2 can transfer to the graphene surface, resulting in the inhibition of the recombition of the holes and electrons, thereby leading to the improvement of photocatalytic efficiency. But the activity of the G_1-TiO_2 composites was the most highest, the degradation process has been completed within 25 minutes. As the content of the graphene oxide in the composite was increased, more TiO_2 nanoparticles were directly anchored onto the graphene oxide sheets. In addition, the increase of the graphene oxide content in the composites could improve the adsorption capability of the composites. However, the black graphene oxide sheets in the composite will increase photo absorbing and scattering, leading to a decrease of the photocatalytic activity of the composites when the graphene oxide content was too high. The TiO_2 nanocrystals are firmly fixed on the surface of GAs, owing to a strong interaction between them, which is also responsible for the high photocatalytic performance of TiO_2/GAs.

2.3. Lithium-ion battery anode

To confirm the TiO_2/GAs Hollow Nanocrystals is beneficial for lithium insertion/extraction properties and the storage of lithium ions. The Figure 7a, b shows the representative cyclic voltammograms (CVs) of the LIBs made with G_1-TiO_2 and pure TiO_2. Looking at the symmetry of the CV curves, we can confirm the very similar Li-ion insertion/deinsertion capability inside the composits, revealing a good reversibility of the process. Fig. 8 presents the cycling performance of different electrodes at constant current densities of 0.5 C. It is clear that specific capacity of the G1-TiO_2 (168.5$mAhg^{-1}$) is the highest among the other prepared materials, which values near to the theoretical capacity of bulk titania (168 $mAhg^{-1}$).

Fig. 9 presents the rate capability of the anode materials tested from 0.5 to 10 C with identical discharge and charge current density and twenty discharge/ charge cycles at each rate, The reversible capacity of the G_1-TiO_2 composites is as high as 160.7mAh g^{-1} after 120 cycles at the current density of 0.5 C (1 C=168 mAg^{-1}) , which is higher than those TiO_2/GAs composites from $G_{0.5}$-TiO_2 (80.4 $mAhg^{-1}$), G_2-TiO_2 (83.2$mAhg^{-1}$), G_5-TiO_2 (119.9$mAhg^{-1}$) and pure TiO_2 (124.5 $mAhg^{-1}$) . The initial specific capacity of G_1-TiO_2 composites approaches 157 $mAhg^{-1}$ at low 0.5 C rate. The capacity retention is satisfactory. The capacity of these materials can be to 76 $mAhg^{-1}$ and 56 $mAhg^{-1}$ at 5 C and 10 C current rates, respectively. Thus, the cell operates with the expected potential profiles delivering a sufficient reaction of the theoretical capacity even at very high rates as high as 10 C. The decrease in the specific capacity observed when increasing the current rate can, in general, be attributed to limitations in the Li+ ion diffusion and in the electron transport through the porous nature of the active material grains. This result indeed confirms that the graphene in the hybid material is effective in improving high performance of the electrode materials. The cycle response is also encouraging since the Coulombic efficiency following the first cycles, which is nearly above 99% and, subsequently, remains highly stable throughout the cycles, indicating excellent reversible cycling (Fig. 10).

To further testify the enhanced electronic conductivity, electrochemical impedance spectroscopy measurements on G_1-TiO_2 composites and pure TiO_2 materials were performed after cycles. The Nyquist plots of the G_1-TiO_2 composites and pure TiO_2 (Fig. 11) all show depressed semicircles at high frequencies. We estimate that the resistivity of the cells decreased from 127.4 Ω for the pure TiO_2

to 62.83 Ω with the addition of only 1.0wt % graphene. The highly conductive graphene sheets can facilitate electron transfer and thus decreasing resistance. Therefore, improved high charge rate performance could be attributed to the substantial decrease in charge-transfer resistance.

3. Conclusion

In summary, we use a facile one-step hydrothermal method to prepare hollow nanocrystals TiO_2/ Graphene nanosheets composites. The materials exhibit excellent specific capacity, outstanding lithium storage performance, highly reversible capacity, and excellent rate performance. Among them, TiO_2/ Graphene nanosheets nanocomposite with 1% graphene exhibits the greatest photoelectrical properties and Li-ion insertion/extraction kinetics in TiO_2.

This demonstrates that functionalized graphene sheets are a promising conductive additive for Li-ion battery electrode materials. Besides, both the structure design and the synthesis method provide a wide insight for the synthesis of other materials to improve the performance of electrodes for electrochemical energy storage and conversion.

4. Experimental

Chemicals: All chemicals, including Titanium sulfate ($Ti(SO_4)_2$), Graphite powder (MO), hydrogen peroxide (H_2O_2, 30%), ammonia solution (NH_4OH, 30%), sodium nitrate ($NaNO_3$), potassium permanganate($KMnO_4$), sulfuric acid (H_2SO_4, 97%), Sodium sulfate (Na_2SO_4) and ethanol (C_2H_5OH), were used as received without any further purification and ultrapure water was used for all experiments.

Synthesis of GAs-TiO_2 nanocomposite: Graphene oxide was synthesized using a modified Hummer's method.[27] GAs-TiO_2 nanocomposites with a varying amount of graphene were prepared by one-step hydrothermal method using GO nanosheets and titanium sulfate as the starting materials. The synthesis procedure was as follows: An aqueous solution of $Ti(SO_4)_2$ was added in a vessel. NaOH solution was then added dropwise to the vessel under stirring at room temperature. Gelatinous white precipitate was formed instantly. The resulting precipitate was separated from the mother liquor by centrifugation and washed with distilled water until the absence of residual SO_4^{2-} (tested by the reaction of them with a $BaCl_2$ solution).

A varying amount of GO were dispersed into 30 mL of water and then ultrasonic dispersion at least 60 min at room temperature, after that 0.8 g of gelatinous white precipitate, 6.3 g $LiOH·H_2O$ was added to an aqueous dispersion of GO solution under vigorous stirring and ultrasonication. The weight contents of graphene designated (wt%) in GAs-TiO_2 nanocomposites were 0%, 0.5%, 1%, 2% and 5%, and the corresponding samples were labeled as pure TiO_2 (G_0-TiO_2), $G_{0.5}$-TiO_2, G_1-TiO_2, G_2-TiO_2 and G_5-TiO_2, respectively. Next, the mixtures were transferred into the stainless Teflon-lined autoclave of 50 mL inner volume, and then heated to 130 ^oC for 48 h under autogenous pressure, followed by cooling naturally to room temperature. The precipitates were collected by centrifugation, washed thoroughly with diluted HCl solution and deionized water for three times respectively. Finally, the resulting products were fully dried by lyophilization.

Characterization of materials: X-ray diffraction (XRD) patterns were collected on a Bruker D8 Advance X-ray Diffractometer. The morphologies were characterized by transmission electron microscopy (TEM). High resolution TEM (HRTEM) analysis was performed on a Tecnai G2 S-Twin F20 microscope. The surface morphologies were observed by scanning electron microscopy (JEOL.JSM-6360LV). BET surface area measurements were carried out by N2 adsorption at 77 K using an ASAP2020 instrument.

Photocatalytic studies:The photocatalytic activity of TiO_2/GAs is measured by monitoring the degradation of methylthionine chloride (20 mg/L). The photocatalytic experiments were carried out in a reactor (50 mL) at room temperature (25 ^oC), being filled with an aqueous suspension (30 mL) containing catalyst (30 mg). The suspension was magnetically stirred for 30 min in dark to favor the adsorption–desorption equilibration. The concentration of the substrate after equilibration was measured and taken as the initial concentration (C_0) to discount the adsorption in the dark. At 5 minutes intervals, 4 mL aliquots were sampled, immediately centrifuged at 12000 rpm for 2 min to remove the graphene oxide/TiO_2 particles and the methylthionine chloride solution was analyzed by a visible spectrophotometer at a wavelength of 664 nm. G_0-TiO_2, $G_{0.5}$-TiO_2, G_1-TiO_2, G_2-TiO_2 and G_5-TiO_2 were adopted to compare the photocatalytic activity under the same experimental conditions.

Electrochemical Measurements:The electrochemical experiments were carried out in coin-type cells. All the electrodes were prepared by mixing the hybrids, carbon black (Super-P), and poly-(vinyl difluoride) (PVDF) at a weight ratio of 80:10:10 to form the slurry which was subsequently coated onto a copper foil (99.6 %). Pure lithium foils were used as counter electrodes. The electrolyte consisted of a solution of LiPF6 (1M) in ethylene carbonate (EC)/dimethyl carbonate (DMC) (1:1, by weight percent). The cells were assembled in an Ar-filled glove box with the concentrations of moisture and oxygen below 0.1 ppm. The electrochemical performance was tested at various rates in the voltage range of 1.00–2.50 V at different current rates of 0.5C、0.5C-10C, where 1 C = 168 mAg^{-1}.

Acknowledgements

This work was financially supported by the Postdoctoral Foundation of China and National Science Foundation of China (51275203); the Key Scientific and Technological Project of Jilin Province, Project Grant No. 20140204052GX; Open Project of State Key Laboratory of Inorganic Synthesis and Preparative Chemistry, College of Chemistry, Jilin University (No. 201505).

Notes and references

[a]Key Laboratory of automobile Materials, Ministry of Education, and College of Materials Science and Engineering, Jilin University, Changchun 130025, China e-mail: yukf@jlu.edu.cn

[b]Roll Forging Research Institute, Jilin University, Changchun, 130025, Jilin, China

[c]State Key Laboratory of inorganic Synthesis and Preparative Chemistry, College of Chemistry, Jilin University, Changchun 130012

† Footnotes should appear here. These might include comments relevant to but not central to the matter under discussion, limited experimental and spectral data, and crystallographic data.

Electronic Supplementary Information vailable: [details of any supplementary information available should be included here]. See DOI: 10.1039/b000000x/

1 X.W.D. Lou, L.A. Archer and Z. Yang, *Advanced Materials*. **2008**, **20**, 3987-4019.
2 V. Štengl, D. Popelková and P. Vlácil, *The Journal of Physical Chemistry C*. **2011**, **115**, 25209-25218.
3 M. Xing, J. Zhang, B. Qiu, B. Tian, M. Anpo and M. Che, *Small*, **2015**, **11**: 1920-1929.
4 B. Qiu, M. Xing, Q. Yi and J. Zhang, *Angewandte Chemie*, **2015**, **127**: 10789-10793.
5 S. Kim, S.J. Hwang and W.Y. Choi, *J. Phys. Chem. B*. **2005**, **109**, 24260-24267.
6 N. Sobana, M. Muruganadham and M. Swaminathan, *J. Mol. Catal. A: Chem*. **2006**, **258**,124-132.
7 C. Burda, Y. Lou, X. Chen, A. C. Samia, J. Stout and J. L. Gole, *Nano Letters*. **2003**, **3**, 1049-1051.

8 B Tryba, A.W. Morawski and M. Inagaki, *Applied Catalysis B: Environmental*. **2003**, **41**, 427-433.
9 Y. Yao, G. Li, S Ciston, R. M. Lueptow, and K. A. Gray, *Environmental science & technology*. **2008**, **42**, 4952-4597.
10 K. S. Novoselov, A.K. Geim, S.V. Morozov, D. Jiang, Y. Zhang, S. A. Dubonos and A. A. Firsov, *Science*. **2004**, **306**, 666-669.
11 M.I. Katsnelson, *Mater. Today.* **2007**, **10**, 20-27.
12A.K. Geim, *Science*. **2009**, **324**, 1530-1534.
13 C.N.R Rao, A.K. Sood and K.S. Subrahmanyam, *Angewandte Chemie International Edition*. **2009**, **48**, 7752-7777.
14 C. Lee, X. Wei, J.W. Kysar and J. Hone, *Science*. **2008**, **321**, 385-388.
15 B. Qiu, M. Xing and J. Zhang, *Journal of the American Chemical Society*, **2014**, **136**: 5852-5855.
16 H. Cao, B. Li, J. Zhang, F. Lian, X. Kong and M. Qu, *J. Mater. Chem.* **2012**, **22**, 9759-9766.
17 J. Qiu, P. Zhang, M. Ling, S. Li, P. Liu, H. Zhao and S. Zhang, *ACS Appl. Mater. Interfaces.* **2012**, **4**, 3636-3642.
18 W. Li, F. Wang, S. Feng, J. Wang, Z. Sun, B. Li, Y. Li, J. Yang, A.A. Elzatahry, Y. Xia and D. Zhao, *J. Am. Chem. Soc*. **2013**, **135**, 18300-18303.
19 A.S. Arico, P. Bruce, B. Scrosati, J.M. Tarascon and W. Van Schalkwijk, *Nat. Mater.* **2005**, **4**, 366-377.
20 Q. Zhang, E. Uchaker, S.L. Candelaria and G. Cao, *Chem. Soc. Rev.* **2013**, **42**, 3127-3171.
21 J. Zhang, H. Yang, G. Shen, P. Cheng, J. Zhang and S. Guo, *Chemical Communications.* **2010**, **46**, 1112-1114.
22 P. D. Cozzoli, A. Kornowski and H. Weller, *J. Am. Chem. Soc.* **2003**, **125**, 14539-14548.
23 Y. Wang, Y. Li, L. Tang, J. Lu and J. Li, *Electrochem. Commun.* **2009**, **11**, 889-892.
24 X. Y. Zhang, H. P. Li, X. L. Cui and Y. H. Lin, *J. Mater. Chem*. **2010**, **20**, 2801-2806.
25 Z. Huang, H. Zhou, C. Li, F. Zeng, C. Fu and Y. Kuang, *J. Mater. Chem*. **2012**, **22**, 1781-1785.
26 H. Zhang, X. Lv, Y. Li, Y. Wang and J. Li, *ACS nano*. **2009**, **4**, 380-386.
27 Jr.W.S. Hummers and R. E. Offeman, *J. Am. Chem. Soc*. **1958**, **80**, 1339-1339.

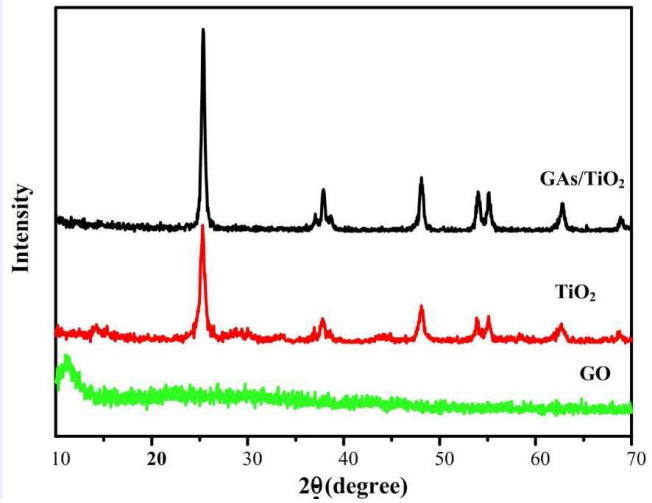

Fig. 1 XRD images of pure TiO_2 and 1.0 wt% GAs/TiO_2 composite.

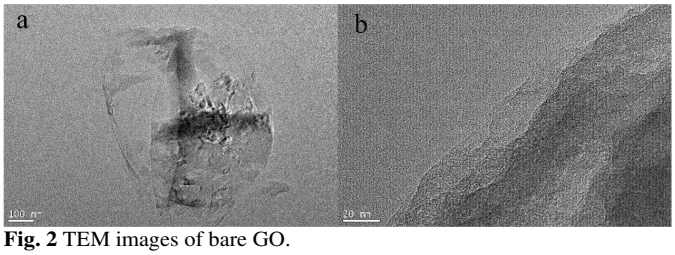

Fig. 2 TEM images of bare GO.

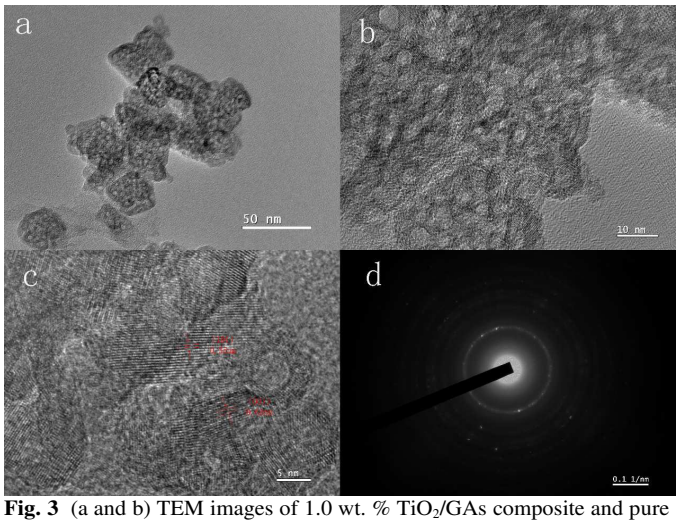

Fig. 3 (a and b) TEM images of 1.0 wt. % TiO_2/GAs composite and pure TiO_2, (c and d) HRTEM and SAED image of TiO_2/GAs (1.0 wt. %).

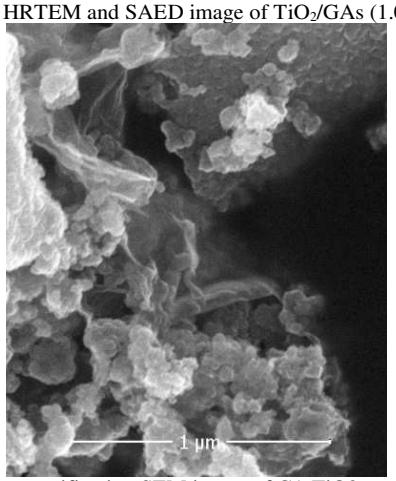

Fig. 4 The high-magnification SEM image of G1-TiO2.

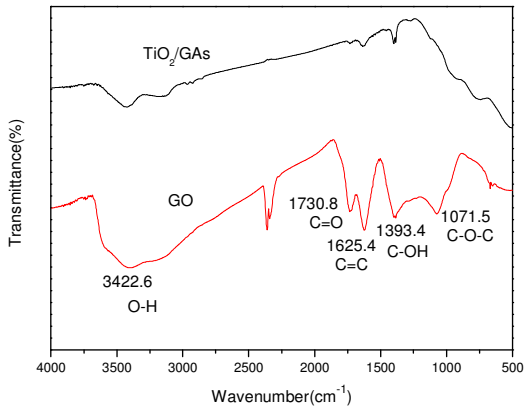

Fig. 5 FTIR spectra of graphite oxide and G_1-TiO_2 hollow nanocrystals, respectively.

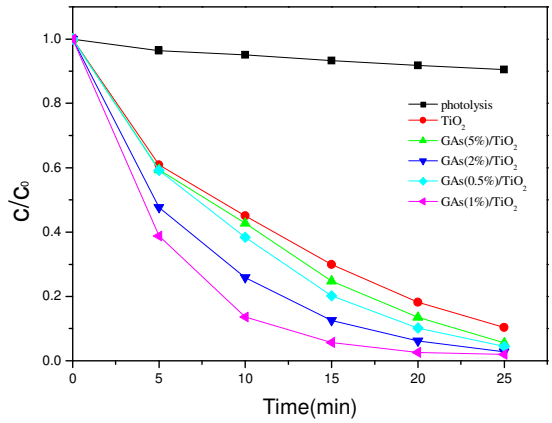

Fig. 6 Photodegradation of Methylthionine chloride by TiO_2/GAs nanocomposite with different weight ratios of graphene under UV light irradiation.

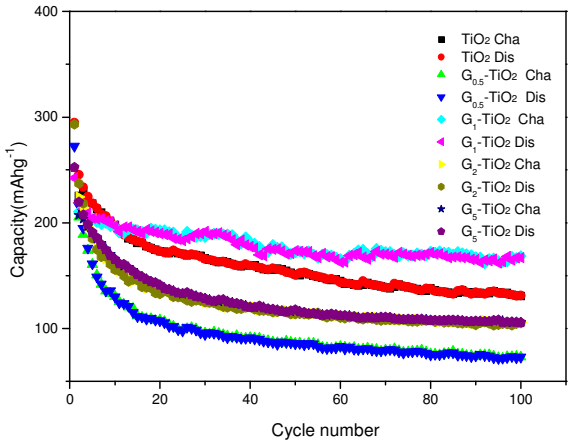

Fig. 8 Cycling performance of the different electrodes at the rate of 0.5 C.

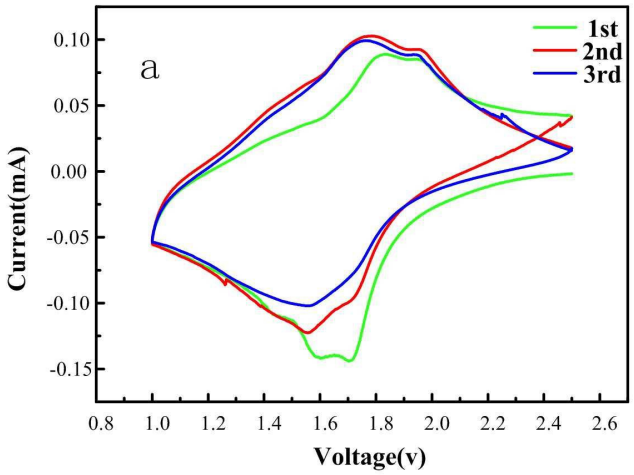

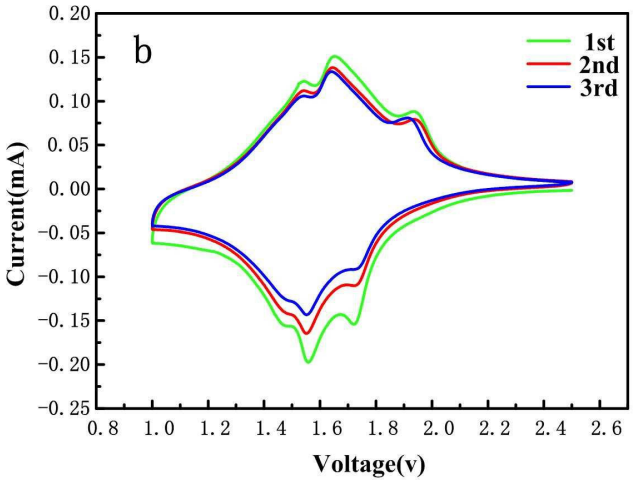

Fig. 7 CVs of the G1- TiO_2 (a) and TiO_2 (b) electrodes from the first cycle to the third cycle at a scan rate of 0.1 mVs−1.

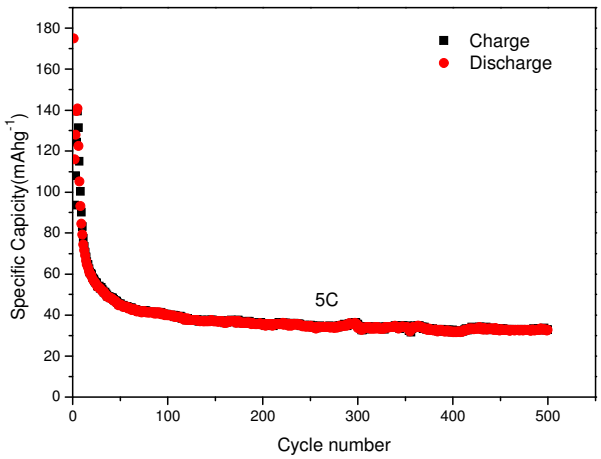

Fig. 9 Durability test at high 5 C current of G_1-TiO_2 composite.

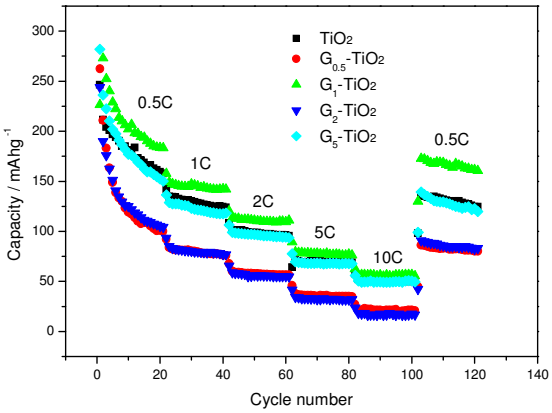

Fig. 10 Rate performance of GAs/TiO_2 nanocomposites and pure TiO_2 at varied current densities

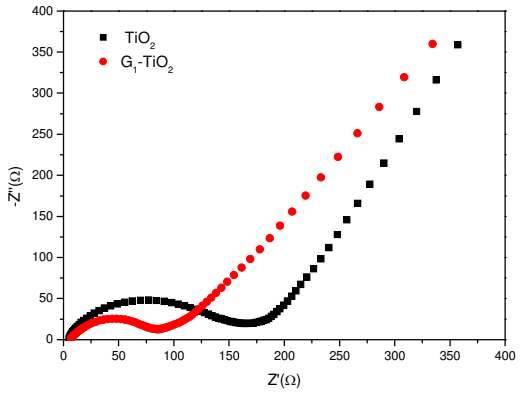

Fig. 11 Nyquist plots of the electrodes of G_1-TiO_2 composite and pure TiO_2.

Graphical Abstract

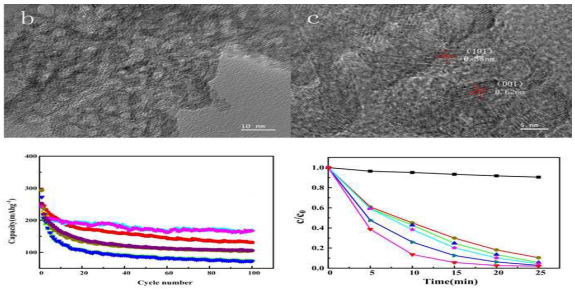

In order to improve photocatalytic and lithium ion batteries performance, we prepare hollow nanocrystals structure by one-step hydrothermal method.